Available online at www.sciencedirect.com

ScienceDirect

Transportation Research Procedia00 (2022) 000–000

Transportation Research Procedia

www.elsevier.com/locate/procedia

Smart transport conference 2022 Conference

Study of the heat transfer efficiency of spring elements for use in transport

Olga Soloveva*, Sergei Solovev, Azalia Talipova, Rozalina Shakurova, Julia Sabirova

Kazan State Power Engineering University, Kazan, 420066, Russia

Abstract

The problem of heat removal in transport is currently urgent. The paper presents a numerical simulation of the airflow of heat exchange elements in the form of springs located at the angles 45° and 90°, with various porosities of the element packaging: $\varepsilon = 0.75$; $\varepsilon = 0.8$; $\varepsilon = 0.85$; $\varepsilon = 0.9$; $\varepsilon = 0.95$. Numerical simulation was carried out in the ANSYS Fluent software (v. 19.2) for various airflow velocities. Analysis of the influence of heat exchange elements and air velocity parameters on the value of energy efficiency was carried out.

Keywords: Transport, springs, heat transfer, numerical simulation, heat flux, energy efficiency

1. Introduction

In almost any apparatus, mechanism, production, processes associated with the release or absorption of thermal energy occur. Heat exchangers are an integral part of cooling systems, including in transport: for oil cooling in diesel and gasoline engines, cooling air entering the cylinders, etc. (Kumar et al., 2018; Soloveva et al., 2020). The operability of the transport depends on the quick delivery or removal of heat.

Analysis of the thermal balance of the engine shows that less than 50% of the energy generated by the combustion of the fuel is output as effective work, and the remaining energy disappears in the form of exhaust gases and engine coolant. Therefore, heat recovery of the exhaust gases will significantly increase the engine's energy efficiency and reduce the total fuel consumption of cars. Automotive thermoelectric exhaust gas generators (AETEG) recover heat from exhaust gases (Pandey and Hansdah, 2021). A high-efficiency heat exchanger is required to extract maximum energy from the engine's exhaust gases while maintaining a pressure drop within acceptable limits and increasing the

* Corresponding author. Tel.: +7-927-401-0999;
E-mail address: solovyeva.ov@kgeu.ru

potential for power generation by a thermoelectric generator. Shi et al. (2022) provide a modified muffler-heat exchanger for combining an exhaust gas heat exchanger and a muffler. The modified noise-suppressed heat exchanger provides improved heat transfer and flow characteristics and more uniform temperature distribution on the hot side. Thus, the exhaust gas pressure drop is reduced by 8.4% compared to the base structure of the muffling heat exchanger by more channels.

The heat exchanger design shall be oriented towards maximum heat transfer while minimizing pressure loss. The use of various methods of intensification of heat exchange in industry and transport has become an important part of the design and development of efficient heat exchangers.

One of the most effective methods for improving heat exchange is using highly porous materials with low weight, low density, and high thermal conductivity (Rashidi et al., 2019). Many scientists studied the thermal characteristics of porous materials (Kopanidis et al., 2010; Hamadouche et al, 2018; Akar et al., 2017; Alvandifar et al., 2018; Soloveva et al., 2021; Soloveva et al., 2021; Soloveva et al., 2021; Soloveva et al., 2019). The effect on the heat transfer of factors such as porosity, thickness, and arrangement of the porous insert, the structure, and geometry of the cell of the porous structures, the complete or partial coating of the pipes with a porous material has been investigated.

In the paper (Unger et al., 2020), the authors studied the thermal and flow characteristics of tubular heat exchangers with a new rib design for tube inclination angles of 0°, 20°, 30°, and 40° to the horizontal. The performance evaluation criterion (Pec) is the largest for the tube with serrated integrated pin fin (SIPF) and the lowest for the tube with circular plain fin (CPF). The heat exchanger's greatest heat transfer per unit volume and temperature difference were achieved for the tube with circular integrated pin fin (CIPF) at the maximum tube angle.

We can conclude that methods for improving heat transfer (ribs of various shapes, metal foam) improve the heat transfer rate but at the same time create an additional pressure drop that plays a decisive role in the design of an effective heat exchanger.

The results of numerical and experimental studies show that the shape of the heat exchange elements directly affects the thermal and dynamic characteristics of the heat exchanger. Round pipes are widely used in heat exchange equipment due to the ease of manufacture and withstand high pressure. However, many studies aim to improve thermohydraulic characteristics by replacing round pipes with more streamlined ones. A drop-shaped pipe bundle has shown superiority over a round one in high thermohydraulic characteristics under the same operating conditions (Deeb, 2022). The pressure difference in the cam row of tubes is about 92-93% lower than in the round row of pipes, and as a result, the thermal-hydraulic characteristics of the cam row of tubes are about 5-6 times higher than in the round row of tubes (Bayat et al., 2014).

Luo and Song (2021) proposed a new twisted annular space formed by two oval tubes twisted against each other for a double tube heat exchanger. The results show that a strong secondary flow is created in the new twisted annular space , contributing significantly to heat transfer. The maximum Nusselt number (Nu) and the friction coefficient (f) of the twisted rings individually are 157% and 118%, respectively, more significant than those of the respective straight rings.

In the article (Dang and Wang, 2021), the authors investigated with numerical methods the mechanisms for enhancing convective heat exchange in a pipe with a new kind of spiral coil insert. Under the same operating conditions, the heat transfer of the helical coil tube is much higher than that of the smooth pipe. The same conclusion was reached in work (Kareem and Shehab, 2021), in which cases of the location of four, six, and eight coil springs, in addition to a smooth (without springs) tube body, were modeled inside the tube side of the double-tube heat exchanger. Numerical results showed that the overall heat transfer coefficient increased by about 14%, 18.7%, and 21.4% for models with 4, 6, and 8 springs, respectively, compared to a smooth tube housing. In a model with 8 springs, a pressure drop was about 2.1 times greater than in a smooth tube.

Thus, we can conclude that after the spring-shaped direction of the heat exchange element, the liquid/air flow begins to rotate, the centrifugal force generated by the tangential velocity increases. Centrifugal force pushes the liquid/air in the central area of heat exchanger housing to the wall area, and liquid/air in the wall area moves to the central area of housing. In this process, longitudinal vortices are formed, and heat transfer characteristics are improved.

The task of this work is a numerical analysis of the effect of the angle and porosity of the package of heat exchange elements in the form of springs on the value of the pressure drop and heat flux.

The studies can form the basis for developing industrial heat exchangers with higher efficiency and lower costs.

Nomenclature	
ε	porosity
Q	heat flux
Δp	pressure drop
E	energy efficiency factor
v	velocity of the air

2. Materials and Methods

We considered airflow of heat exchange elements in the form of springs. We created models of heated elements, placed at angles 45° and 90°, with different values of the porosity of the package: $\varepsilon = 0.75$; $\varepsilon = 0.8$; $\varepsilon = 0.85$; $\varepsilon = 0.9$; $\varepsilon = 0.95$. The dimensions of each element: wire thickness – 1 mm, spiral diameter – 5 mm, step – 5 mm (Fig. 1).

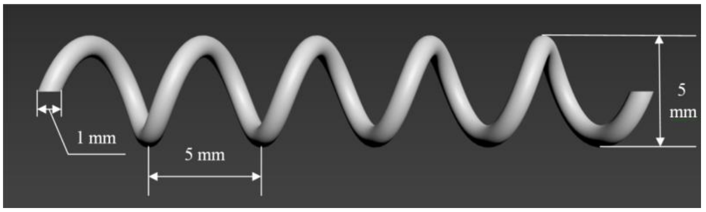

Fig. 1. Dimensions of one heat exchange element.

The computational area is a circular channel with a diameter of 20 mm with heated elements located in it with a length of 20 mm, the length of the inlet and outlet nozzles are 20 and 60 mm, respectively. Such dimensions are due to the need to ensure the distance of the inlet and outlet boundaries for desired convergence of the numerical calculation. Examples of design areas for elements at angles 45° and 90° are shown in Fig. 2 (a, b).

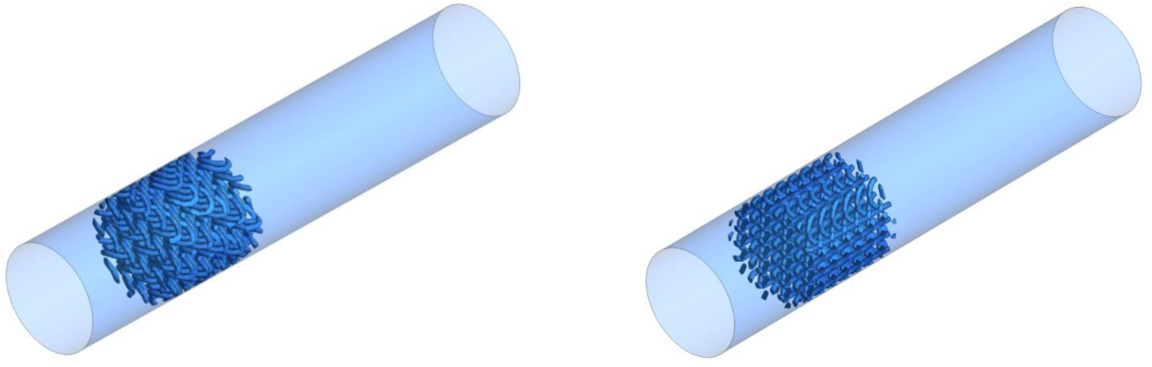

(a) (b)

Fig. 2. Example of the computational area with heat exchange elements in the form of springs arranged at the angle 45° (a) and the angle 90° (b), with porosity of packing of elements 0.8.

Numerical modeling was carried out in the ANSYS Fluent software (v. 19.2). The calculations used an SST model of turbulence. The analysis is carried out at different velocity (therefore, for different mass flow rates): 0.01; 0.05; 0.25; 0.5; 0.75; 1; 1.25 m/s.

The number of grid partitioning cells ranges from 8.5 to 30.7 million. We set the following discrepancy values: continuity – $1\cdot10^{-13}$; x-velocity, y-velocity, z-velocity, energy, k, omega, intermit, retheta – $1\cdot10^{-6}$.

At the inlet, we set the air temperature to 293 K, and the temperature on the surface of the element is 373 K.

Air parameters used in calculations (calculated in Fluent): density – $\rho = 1.225$ kg/m^3; dynamic viscosity – $\mu = 1.7894\times10^{-5}$ kg/(m·s); mass flow rates at airflow velocities: 0.01 m/s – $G = 3.84\times10^{-6}$ kg/s; 0.05 m/s – $G = 1.92\times10^{-5}$ kg/s; 0.25 m/s – $G = 9.60\times10^{-5}$ kg/s; 0.5 m/s – $G = 1.92\times10^{-4}$ kg/s; 0.75 m/s – $G = 2.88\times10^{-4}$ kg/s; 1 m/s – $G = 3.84\times10^{-4}$ kg/s; 1.25 m/s – $G = 4.80\times10^{-4}$ kg/s.

The purpose of this work is to determine the effect of the angle of location and porosity of the package of heat exchange elements on the value of heat flux and energy efficiency factor.

Energy efficiency factor is calculated by formula (Liu et al., 2020):

$$E_F = \frac{Q}{\delta P}, \tag{1}$$

where Q is the heat flux from the feature surface, W; δP is the power spent on coolant (air) pumping, W:

$$\delta P = G_V \cdot \Delta p = \frac{G}{\rho} \cdot \Delta p$$

where G_V is the volumetric airflow rate, m^3/s; Δp is the pressure drop, Pa; G is the mass airflow rate, kg/s; ρ is the air density, kg/m^3.

3. Results

Figure 3 shows graphs of changes in heat flux depending on the air velocity. When the porosity of the package of elements is equal, the heat flux from the surface of the springs is located at the angle 45°, higher than from the surface of the springs located at the angle 90°, except in the following cases: 1 – at porosity $\varepsilon = 0.75$ at the velocity of air of 0.05 m/s to the springs placed at an angle 90° there correspond values of a heat flux 0.23% higher, than to the springs placed at the angle 45°; 2 – at porosity $\varepsilon = 0.8$ at the velocity of air of 0.01 m/s – is 0.46% higher; 3 – at porosity $\varepsilon = 0.9$ at the velocity of air of 0.01 m/s – is 1.80% higher; 4 – at porosity $\varepsilon = 0.95$ at the velocity of air of 0.01 m/s – is 0.71% higher. The higher porosity, the greater the increase in the heat flux value of the springs located at an angle of 45° relative to the springs located at an angle of 90°.

Figure 4 shows the pressure drop curves depending on the velocity at the porosity of the packing elements: $\varepsilon = 0.75$; $\varepsilon = 0.8$; $\varepsilon = 0.85$; $\varepsilon = 0.9$; $\varepsilon = 0.95$. The graphs show that the elements placed at an angle of 90°, correspond to the smallest values of the pressure drop at all design velocities and values of the porosity of the package of elements, except for the velocity of 0.01 m/s at porosity $\varepsilon = 0.8$ and velocities 0.01 and 0.05 m/s at porosity $\varepsilon = 0.85$. In these cases, springs placed at an angle of 45° correspond to a pressure drop of less than 4.96; 9.45 and 26.19%, respectively, than springs placed at an angle of 90°.

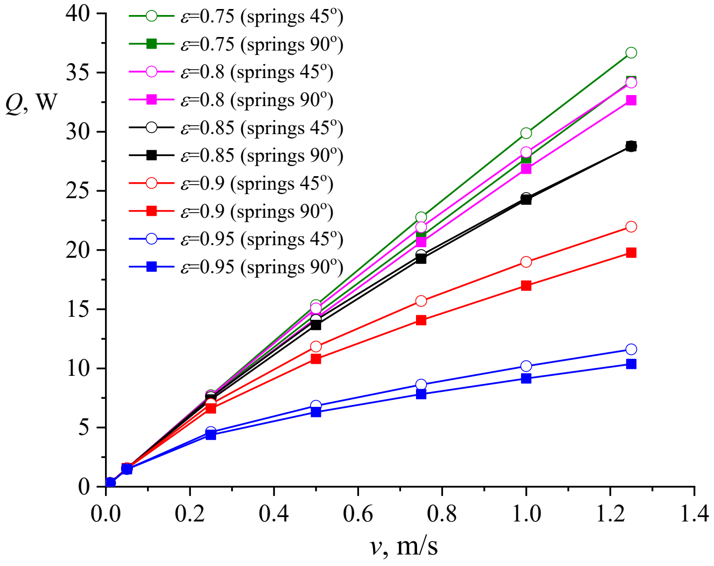

Fig. 3. Change of heat flux depending on air velocity for element packing porosities: $\varepsilon = 0.75$; $\varepsilon = 0.8$; $\varepsilon = 0.85$; $\varepsilon = 0.9$; $\varepsilon = 0.95$.

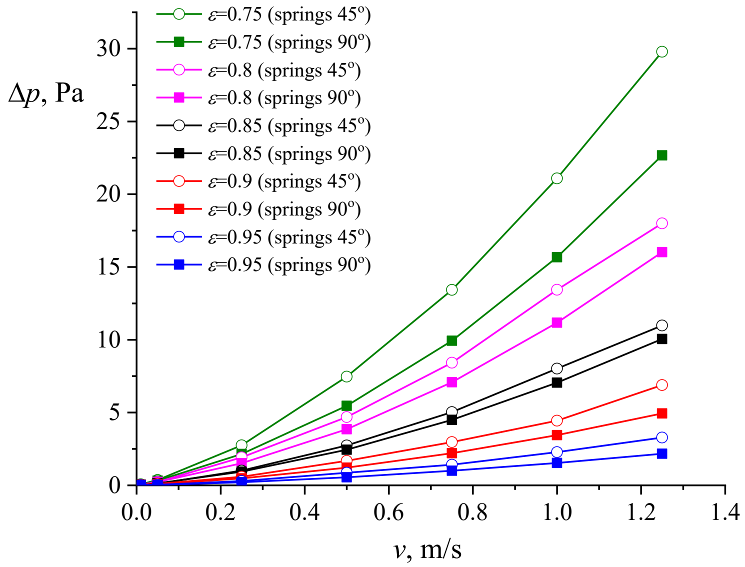

Fig. 4. Change of pressure drop depending on air velocity for element packing porosities: $\varepsilon = 0.75$; $\varepsilon = 0.8$; $\varepsilon = 0.85$; $\varepsilon = 0.9$; $\varepsilon = 0.95$.

Studies of the change in energy efficiency factor (1) depending on the velocity (Fig. 5) showed that at the porosity of the packages of elements $\varepsilon = 0.75$; $\varepsilon = 0.9$ and $\varepsilon = 0.95$ the greatest values at all rated velocities show the springs placed at an angle 90°. With the porosity of the packing of elements $\varepsilon = 0.8$ at a velocity of 0.01 m/s, the highest energy efficiency value corresponds to springs placed at an angle of 45°. This is due to the lower value of pressure drop at given velocity for springs located at an angle of 45°. With porosity $\varepsilon = 0.85$ at velocities of 0.01 and 0.05 m/s, the highest energy efficiency value also corresponds to springs placed at an angle of 45°. The reasons for this are a higher heat flux value and a lower pressure drop value at these velocities for springs placed at an angle of 45°.

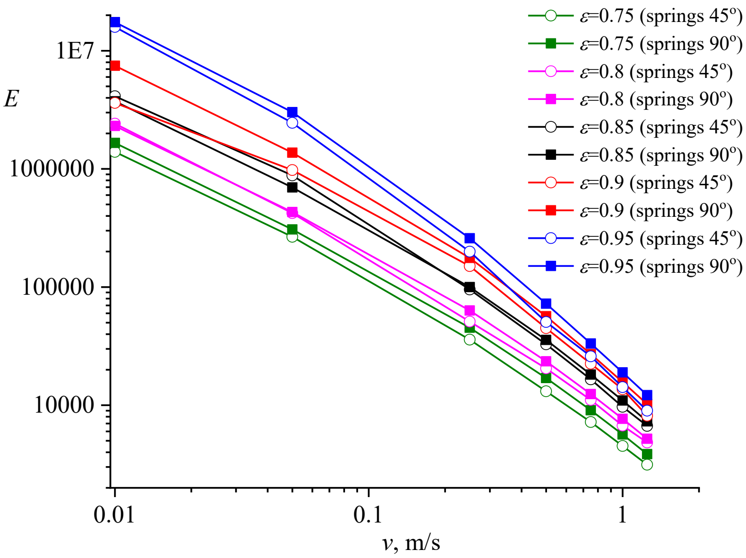

Fig. 5. Change of energy efficiency factor depending on air velocity for element packing porosities: $\varepsilon = 0.75$; $\varepsilon = 0.8$; $\varepsilon = 0.85$; $\varepsilon = 0.9$; $\varepsilon = 0.95$.

Figure 6 (a-e) shows an increase in energy efficiency when using springs placed at an angle of 90° relative to springs placed at an angle of 45°.

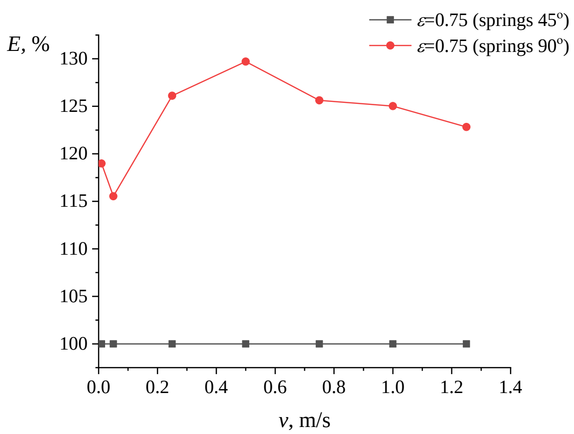

(a)

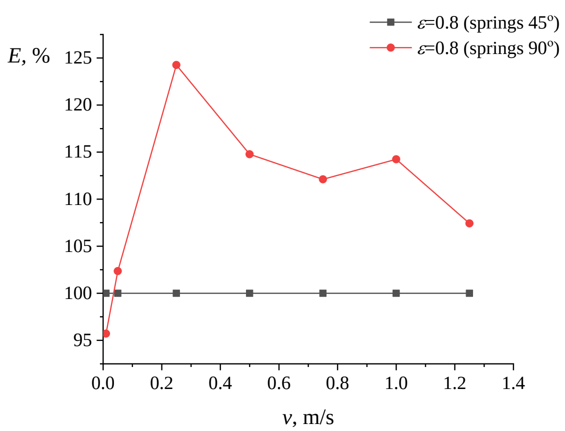

(b)

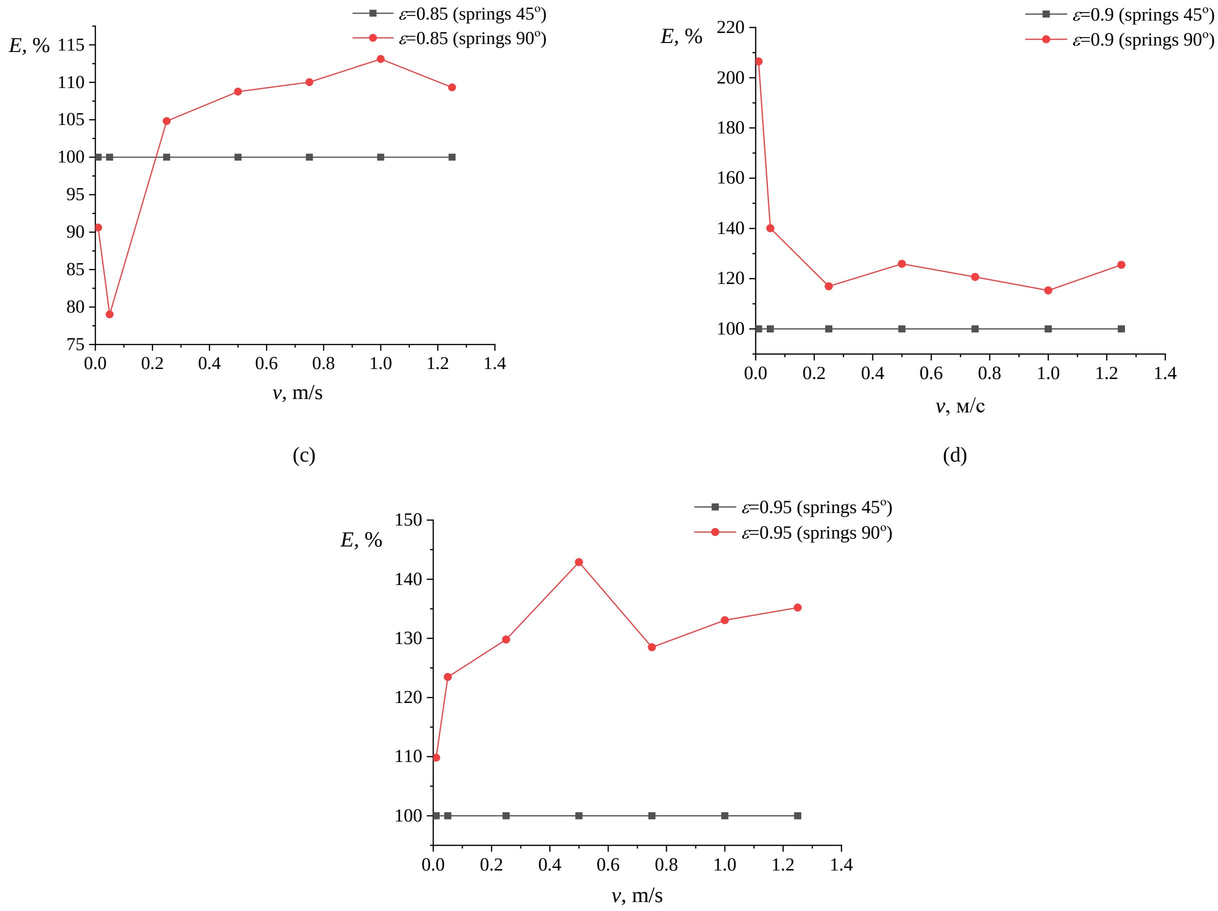

(e)

Fig. 6. Change of energy efficiency factor depending on air velocity in percent relative to springs placed at angle 45° for porosities of elements packing: (a) $\varepsilon = 0.75$; (b) $\varepsilon = 0.8$; (c) $\varepsilon = 0.85$; (d) $\varepsilon = 0.9$; (e) $\varepsilon = 0.95$.

4. Conclusion

In the presented work, we studied the airflow of heat exchange elements in the form of springs arranged at angles 45° and 90° at different values of porosities of element packaging: $\varepsilon = 0.75$; $\varepsilon = 0.8$; $\varepsilon = 0.85$; $\varepsilon = 0.9$; $\varepsilon = 0.95$. We found that elements placed at an angle of 45° in most cases correspond to the highest value of heat flux at the analyzed porosities and flow velocities due to greater contact with the air surface. Elements placed at an angle of 90° correspond to the lowest values of the pressure drop at all design velocities and values of the porosity of the package of elements, except for the velocity of 0.01 m/s at porosity $\varepsilon = 0.8$ and velocities of 0.01 and 0.05 m/s at porosity $\varepsilon = 0.85$. When the porosity of the packages of elements $\varepsilon = 0.75$; $\varepsilon = 0.9$, and $\varepsilon = 0.95$, the greatest values of energy efficiency factor at all rated velocities show the springs placed at an angle 90°. With the porosity of the packing of elements $\varepsilon = 0.8$ at the velocity of 0.01 m/s, the highest energy efficiency value corresponds to springs placed at an angle of 45°. With a porosity $\varepsilon = 0.85$ at velocities of 0.01 and 0.05 m/s, the highest energy efficiency value also corresponds to springs placed at an angle of 45°.

Acknowledgments

The research was funded by the Russian Science Foundation, grant number 21-79-10406, https://rscf.ru/en/project/21-79-10406/

References

Kumar, B., Srivastava, G., Kumar, M., Patil, A.K., 2018. A review of heat transfer and fluid flow mechanism in heat exchanger tube with inserts. Chem. Eng. Process. 123, 126-137.https://doi.org/10.1016/j.cep.2017.11.007

Soloveva, O. V., Solovev, S. A., Khusainov, R. R., Yafizov, R. R., 2020. Investigation of hydrodynamics and convection in the porous car heat exchanger. IOP Conf. Ser. Mater. Sci. Eng.918(1), 1-6. https://doi.org/10.1088/1757-899X/918/1/012169

Pandey, A., Hansdah, D., 2021. Heat exchangers for automotive exhaust thermoelectric generators: A review. AIP Conf Proc. 2341(1), 1-17.https://doi.org/10.1063/5.0050132

Shi, L., Xu, W., Ma, X., Wang, X., Tian, H., Shu, G., 2022. Thermal and acoustic performance of silencing heat exchanger for engine waste heat recovery. Appl. Therm. Eng. 201, 1-12. https://doi.org/10.1016/j.applthermaleng.2021.117711

Rashidi, S., Kashefi, M.H., Kim, K.C., Samimi-Abianeh, O., 2019. Potentials of porous materials for energy management in heat exchangers – A comprehensive review. Appl. Energy. 243, 206-232.https://doi.org/10.1016/j.apenergy.2019.03.200

Kopanidis, A., Theodorakakos, A., Gavaises, E., Bouris, D., 2010. 3D numerical simulation of flow and conjugate heat transfer through a pore scale model of high porosity open cell metal foam. Int. J. Heat Mass Transf. 53, 2539-2550.https://doi.org/10.1016/j.ijheatmasstransfer.2009.12.067

Hamadouche, A., Azzi, A., Abboudi, S., Nebbali, R., 2018. Enhancement of heat exchanger thermal hydraulic performance using aluminum foam. Exp. Therm. Fluid Sci. 92, 1-12.https://doi.org/10.1016/j.expthermflusci.2017.10.035

Akar, S., Rashidi, S., Esfahani, J.A., 2017.Appropriate position of porous insert in a heat exchanger by thermohydraulic analysis. Heat Transf. - Asian Res. 46, 1363-1379.https://doi.org/10.1002/htj.21279

Alvandifar, N., Saffar-Avval, M., Amani, E., 2018. Partially metal foam wrapped tube bundle as a novel generation of air cooled heat exchangers.Int. J. Heat Mass Transf.118, 171-181.https://doi.org/10.1016/j.ijheatmasstransfer.2017.10.104

Soloveva, O., Solovev, S., Zaripova, R., Khamidullina, F., Tyurina, M., 2021. Evaluation of the effective porosity of an open cell foam material for using in heat and mass transfer numerical simulations. E3S Web Conf. 258, 1-6. https://doi.org/10.1051/e3sconf/202125811010

Soloveva, O., Solovev, S., Yafizov, R., 2021. Hydrodynamics and Convective Heat Transfer in Open Cell Foam with Micropores. Transp. Res. Proc. 54, 64-68. https://doi.org/10.1016/j.trpro.2021.02.048

Soloveva, O., Solovev, S., Khaibullina, A., Yafizov, R., 2021. Method of the Wastewater Treatment in Transport Using a Porous Material. Transp. Res. Proc. 54, 712-718. https://doi.org/10.1016/j.trpro.2021.02.124

Soloveva, O., Solovev, S., Khusainov, R., Yafizov, R., 2019. Mathematical modelling of heat transfer in open cell foam of different porosities. Adv. Intell. Sys. Comput. 1259, 371-382. https://doi.org/10.1007/978-3-030-57453-6_33

Unger, S., Beyer, M., Szalinski, L., Hampel U., 2020. Thermal and flow performance of tilted oval tubes with novel fin designs. Int. J. Heat Mass Transf. 153, 1-13.https://doi.org/10.1016/j.ijheatmasstransfer.2020.119621

Deeb, R., 2022. Numerical analysis of the effect of longitudinal and transverse pitch ratio on the flow and heat transfer of staggered drop-shaped tubes bundle. Int. J. Heat Mass Transf. 183, 1-23.https://doi.org/10.1016/j.ijheatmasstransfer.2021.122123

Bayat, H., Lavasani, A. M., Maarefdoost, T.,2014. Experimental study of thermal–hydraulic performance of cam-shaped tube bundle with staggered arrangement. Energy Convers. Manag. 85, 470-476.https://doi.org/10.1016/j.enconman.2014.06.009

Luo, C., Song, K., 2021. Thermal performance enhancement of a double-tube heat exchanger with novel twisted annulus formed by counter-twisted oval tubes. Int. J. Therm. Sci. 164, 1-14. https://doi.org/10.1016/j.ijthermalsci.2021.106892

Dang, W., Wang, L. B., 2021. Convective heat transfer enhancement mechanisms in circular tube inserted with a type of twined coil. Int. J. Heat Mass Transf. 169, 1-14. https://doi.org/10.1016/j.ijheatmasstransfer.2021.120960

Kareem, H. H., Shehab, S. N., 2021. Heat convection enhancement of heat exchanger with cylindrical spring inserts: A numerical analysis. J. Mech. Eng. Res. Dev. 44(7), 370-381.

Liu, X, Zhang, S, Zhou, Z, Zheng, H, Wang, C, Shi, H, Li, M., 2020. Study on structure optimization of heat exchanger and evaluation index of heat transfer performance. HuagongXuebao/CIESCJ. 71(S1), 98-105.https://doi.org/10.11949/0438-1157.20191189